Spring 5-2018

Defining the Role of IP3R-Medicated ER Calcium Flux in JC Polyomavirus Infection

Ashley N. Soucy
University of Maine

DEFINING THE ROLE OF IP_3R-MEDICATED ER CALCIUM FLUX IN JC POLYOMAVIRUS INFECTION

by

Ashley N. Soucy

A Thesis Submitted in Partial Fulfillment
of the Requirements for a Degree with Honors
(Biochemistry)

The Honors College

University of Maine

May 2018

Advisory Committee:

Melissa Maginnis, Ph.D., Assistant Professor of Microbiology, Advisor
Julie Gosse, Ph.D., Associate Professor of Biochemistry
Samuel Hess, Ph.D., Professor of Physics
Keith Hutchison, Ph.D., Professor Emeritus of Biochemistry and Molecular Biology
Sally Dixon Molloy, Ph.D., Assistant Professor of Genomics

ABSTRACT

The human JC polyomavirus (JCPyV) persists as an asymptomatic infection in the kidneys of healthy individuals within the majority of the global population. Viral infection of JCPyV is established through peroral transmission due to poor sanitary practices. In severely immunocompromised individuals, JCPyV migrates to the central nervous system (CNS), resulting in the fatal and incurable demyelinating disease progressive multifocal leukoencephalopathy (PML). Virus-host cell interactions regulate infectious processes and influence viral pathogenesis. JCPyV attachment to host cells is mediated by α2,6-linked LSTc while internalization is mediated by 5-hydroxytryptamine serotonin type 2 receptors (5-HT_2Rs). Activation of 5-HT_2Rs can induce intracellular calcium (Ca^{2+}) release upon ligand binding to activate the inositol triphosphate receptor (IP_3R) signaling pathways. The goal of this project was to determine the role of intracellular Ca^{2+} flux in JCPyV infection. JCPyV induces Ca^{2+} flux from the ER almost immediately upon infection. Limiting Ca^{2+} release from the ER by inhibition of the IP_3R with chemical antagonists significantly reduced JCPyV infection in both human kidney and brain cells, demonstrating a dependence on Ca^{2+} flux to regulate JCPyV infection. Although, JCPyV-induced Ca^{2+} flux occurs at times consistent with viral attachment and entry, analyses of these steps by flow cytometric assays, revealed that JCPyV attachment and entry were not affected by modulation of Ca^{2+} flux. These findings demonstrate that Ca^{2+} flux is regulated upon JCPyV infection and provide important insights into the activation of signaling pathways to drive the infectious process. In the future, this work can increase our understanding of PML pathogenesis and aid in the development of novel PML therapeutics.

ACKNOWLEDGEMENTS

I would like to recognize and express gratitude towards those who have made this research possible. First, I offer a sincere thank you to The University of Maine Honors College for the Junior Year and Thesis INBRE Functional Genomics Fellowships, the Frederick H. Radke Undergraduate Research Fellowship, the INBRE Summer Functional Genomics Fellowship, the Center for Undergraduate Research Summer Fellowship, and the NIH-NIGMS grant (P20GM103423). These programs provided the funding and resources necessary to conduct this research, provided me with this research opportunity, and helped me to mature as a biomedical scientist.

This work was also made possible through the endless support provided by my parents, Kathy and James, and my sister Madeline. Without their constant encouragement and guidance, I would not be the person I am today.

I want to thank Jonah Paris for his relentless encouragement, understanding, and patience that he has shown me through this entire process and the past three years at the University of Maine.

I want to thank all past and current members of the Maginnis Laboratory. Throughout the past four years of my undergraduate experience, this group has become my second family; I have been truly blessed to get to know each and every one of them. This special group of students took the extra time to teach me, answer my questions, and were always eager to lend a helping hand.

I thank my committee members for their insights and guidance through this entire process. Their extensive knowledge on this research topic helped provide direction for this project.

Finally, I would like to recognize the irreplaceable role that Dr. Melissa Maginnis has played in my undergraduate experience. Dr. Maginnis provided me with a rich environment to grow in as an individual, an academic, and a scientist. Her continuous support and passion in the field has shown me what it means to be a successful, resilient, and dedicated scientist. I will never be able to express the amount of gratitude and respect that I have for Dr. Maginnis; I have been very fortunate to have her as my mentor.

TABLE OF CONTENTS

LIST OF FIGURES

INTRODUCTION

Overview

Defined as obligate intracellular parasites, viruses are comprised of either an RNA or DNA genome, which is surrounded by a capsid composed of viral proteins, and sometimes a lipid envelope which encases the capsid[1]. For a virus to replicate, it must invade a host cell that is both susceptible and permissive to infection, as viruses usurp host cell machinery to mediate their replication and cause disease[2]. As a result, the host immune system develops specialized mechanisms to identify and destroy invading pathogens. A body's first line of defense against invading pathogens are physical barriers such as epithelial tissues, stomach acid, and saliva[3]. To combat these defenses, pathogens have evolved to interact with cellular receptors and trick the host into internalizing them. Once inside, however, the pathogen must inhibit the activation of host intrinsic, innate,

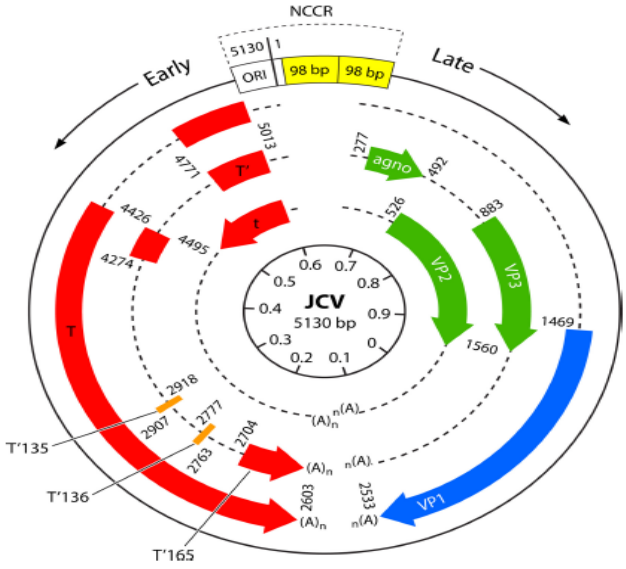

Figure 1. Schematic of JCPyV genome: early and late genes. The non-coding control region (NCCR) contains the open reading frame (ORF) for the early genes (counter clockwise) and late genes (clockwise). The early genes include large T antigen (TAg) while the late gene include structural proteins such as viral protein 1 (VP1). Used with permission from Ferenczy et al. 2012. *Clinical Microbiology*

and adaptive immune responses to avoid destruction[1]. Due to the efficiency of the host immune system, some viruses are only capable of inducing disease once the immune system has been suppressed and are therefore defined as opportunistic viruses[1].

In 1971, a novel opportunistic virus was isolated from a patient suffering from progressive multifocal leukoencephalopathy (PML) and was named the human JC polyomavirus (JCPyV) after the patient's initials[4]. The human JCPyV is non-enveloped with a capsid comprised of three viral proteins (VP1, VP2, VP3) and is ~45 nm in diameter[5]. The genome is circularized double stranded DNA containing one set of early and late-transcribed genes with a total length of 5130 base pairs (Figure 1)[6]. However, while the physical properties of JCPyV have been well examined, the infectious lifecycle of the virus remains poorly understood.

JCPyV is thought to be transmitted via peroral transmission during early childhood due to poor sanitation practices, as it is shed in the urine and can be found in untreated wastewater[7,8]. Data based on recent serological studies suggest that at least 50-80% of the human population is infected with JCPyV[9]. In healthy individuals, JCPyV establishes itself as an asymptomatic infection in the kidney and remains there as a lifelong, persistent infection controlled by the patient's immune system[8]. When an individual becomes severely immunocompromised due to HIV infection, or through the use of immunosuppressive therapies for immune-mediated diseases like multiple sclerosis (MS), JCPyV can migrate from the kidney to the central nervous system (CNS)[10]. Within the CNS, JCPyV can infect the glial cells, astrocytes and oligodendrocytes, and result in their lytic destruction. These cells are critical for the production and maintenance of myelin within the brain and are necessary for healthy

brain function[5]. The destruction of the myelin-producing cells leads to severe demyelination, resulting in a disease called progressive multifocal leukoencephalopathy (PML)[11].

Due to gaps in our knowledge concerning viral-host cell interactions there are no effective therapies or treatments for either JCPyV infection or PML. As a result, the disease proves fatal to the majority of patients within 1 year of symptom onset[4]. To develop successful treatments, it is imperative to first understand the viral-host cell interactions that allows the virus to evade the immune system, persist within the host, and eventually become the etiological agent for PML. Further research investigating the signaling pathways that regulate these viral-host cell interactions in JCPyV infection will provide necessary insights into the infectious lifecycle and could serve as a platform for the development of effective treatments for populations at risk for PML.

Progressive multifocal leukoencephalopathy

While JCPyV was originally isolated in 1971, the first descriptions of PML were noted as early as 1930, and officially defined as a novel disease in 1958[4,14]. The fatal disease was identified due to the destruction of the oligodendrocytes along with morphological changes in astrocytes and oligodendrocytes[4]. PML has an incidence rate (5-10%) in AIDS patients and is described as an AIDS defining illness[15]. Due to the increased use of immunosuppressive therapies for immune-mediated diseases like MS and Crohn's disease, the incidence of PML has increased in these populations[15]. However, due to a lack of effective treatments for JCPyV infection or PML, the best options for patients are to treat the underlying immunosuppression by administering highly active antiretroviral therapy (HAART) for those infected with HIV or cease

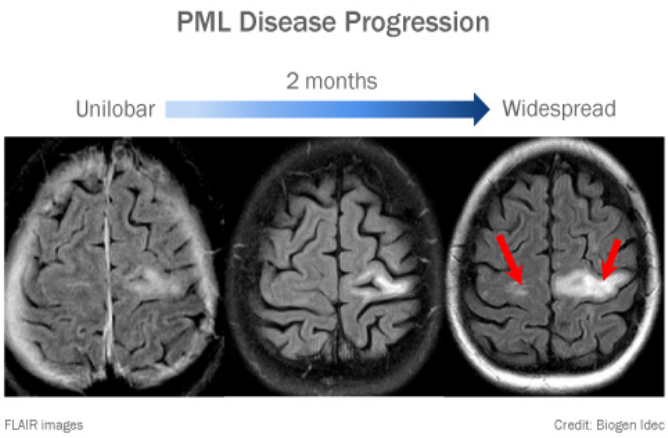

Figure 2. Images of PML lesions and rapid disease progression. Magnetic resonance imaging scans utilizing 3D Flair techniques. White matter located in the brain marks the development of plaques over 2-months. Red arrow points to areas of PML lesions. Image credit: Biogen Idec.

immunomodulatory therapies for the preexisting disease like MS[16]. As a result, therapies are ranked in classes based upon their likelihood to increase a patient's risk of developing PML[4]. The risk stratification is calculated based upon the risks and benefits to the patient by taking the therapy and ensures that patients who are at a high risk of developing this fatal disease are routinely examined[4].

Diagnosis of PML is accomplished through multiple methods. One common methodology is magnetic resonance imaging (MRI) to examine the brain for the loss of myelin, which appears as white plaque regions in the brain or CNS (Figure 2)[7]. In addition to identification of plaques through MRI, the preliminary diagnosis must also be confirmed through the presence of biomarkers, assays determining JCPyV load, and assays for JCPyV mRNA. A strong biomarker for PML in MS patients receiving the drug Natalizumab is CD62L, a selectin present on CD4+ T cells, that has been shown to be expressed at lower levels in patients that develop PML[7]. Patients can also be tested for the presence of JCPyV antibodies and genetic material in urine samples through PCR

techniques [7]. Early detection of JCPyV infection for patients at risk of developing AIDS or beginning immunosuppressive therapies alerts physicians to closely monitor those patients for the development of PML.

Upon disease onset, PML can develop in multiple regions of the brain and often spreads to multiple areas[17]. As a result, there is a wide range of symptoms that may be presented based on which region of the brain is being affected[15]. Classic symptoms can include vision impairment, loss of memory, and hemiparalysis[15]. It is also common for the afflicted individual to experience personality disorders upon symptom onset[8]. Once a patient begins showing clinical symptoms, PML proves fatal to the majority of patients within one year[4]. With no effective therapies or treatments available for either this disease or JCPyV infection, the only option patients receiving immunosuppressive therapies have is to cease immunosuppressive therapies. In doing so, however, patients face the progression of the underlying condition such as cancer, MS, or Crohn's disease[6,8,19]. Additionally, ending immunosuppressive therapies also increases the patient's risk of developing immune reconstruction inflammatory syndrome (IRIS)[18]. IRIS is caused by a rapid return of immune cells within the CNS and results in severe inflammatory responses and worsen the underlying disease condition[18]. Conversely, for individuals with HIV or AIDS initiation of HAART can delay onset of PML[19].

JCPyV infectious lifecycle

Before JCPyV can disseminate through its host and cause PML, it must successfully establish a persistent infection. A successful JCPyV infection is dependent upon the virus encountering a permissive host cell, requiring the cell to have specific functionalities that support viral infection. Research has found that JCPyV initially

attaches to host cells via α2,6 linked sialic acids on lactoseries tetrasaccharide c (LSTc)[12]. This virus-host cell interaction is mediated by the JCPyV capsid protein, viral protein 1 (VP1), which contains multiple binding sites for LSTc[12]. Interestingly, research suggests that in patients diagnosed with PML, VP1 has undergone mutations indicating that these mutations may be required for JCPyV spread from initial sites of infection to the CNS[21]. Following attachment to LSTc, JCPyV requires serotonin receptors to aid in viral infection[23].

Serotonin 5-hydroxytryptamine (5-HT) receptors are seven transmembrane spanning G-protein-coupled receptors[22]. While there are multiple families of 5-HTRs, only the subtype 5-HT_2Rs have been shown to be essential for JCPyV infection[22,23]. Currently, the mechanism by which 5-HT_2Rs mediate JCPyV internalization is poorly understood. However, inhibition of the 5-HT_2Rs inhibits JCPyV infection but has no effect on viral attachment to host cells [23,24]. Interestingly, when 5-HT_2Rs are expressed in human kidney cells, which naturally do not express the receptors but do express LSTc, the cells gain the ability to internalize JCPyV and can become infected[22]. Recent work from the Maginnis Laboratory suggests that JCPyV-mediated activation of 5-HT_2Rs

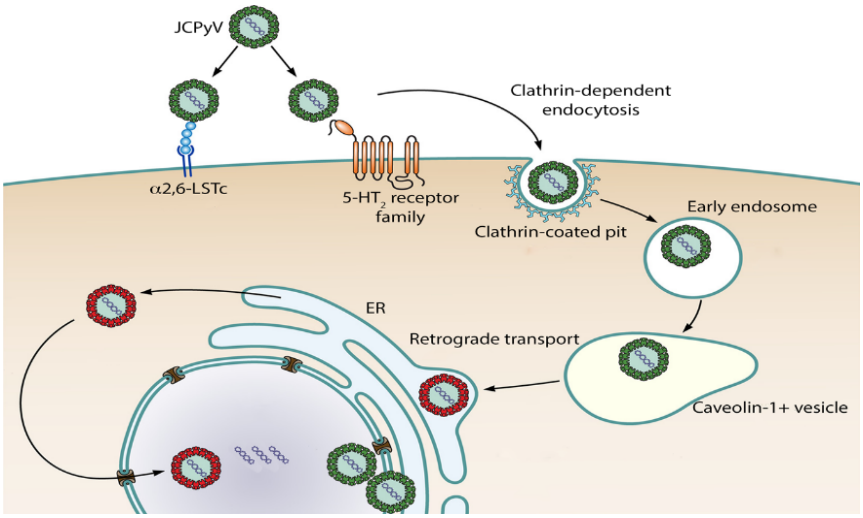

Figure 3. JCPyV internalization and infectivity pathway. JCPyV attaches to α2,6 LSTc receptor and enters cells by 5-hydroxytryptamine receptors (5-HT_2)R through clathrin-mediated endocytosis. JCPyV traffics to early endosomes and cav-1 positive late endosomes, then to the ER where it undergoes uncoating, and enters the nucleus where transcription and replication occur. Used with permission from Maginnis et al. 2015. *J. Neurovirol*. **21,** 601–13.

results in viral internalization via clathrin-mediated endocytosis (Mayberry and Maginnis, unpublished data). This data corroborates the finding, which showed that inhibition of clathrin-mediated endocytosis reduced JCPyV internalization[25]. Once inside the cell, JCPyV traffics through the cytoplasm via endosomes and caveolin-1 vesicles[5]. The virus is then deposited into the endoplasmic reticulum (ER) where the capsid undergoes a partial uncoating event prior to translocation to the nucleus for viral transcription and replication (Figure 3)[26].

Upon arrival in the nucleus, the JCPyV genome is transcribed in a temporally-regulated fashion in which the early genes are transcribed first (Figure 1)[4]. One of the early genes codes for the protein large tumor antigen (large T antigen (T Ag)), which is a major regulator of JCPyV replication[4]. Accumulation of T Ag within the cells promotes the transition from the production of early gene products, to late gene products, including VP1[6]. Additionally, T Ag is capable of binding to host cell DNA to promote its transition from the G_0 to S phase through the activation of host transcription factors[4]. While not all transcription factors required for JCPyV transcription have not been identified, some

have been characterized that play an important role in JCPyV transcription including nuclear factor of activated T cells (NFAT)[28].

NFAT is regulated by the serine/threonine phosphatase calcineurin, which is activated by calcium (Ca^{2+}) flux from the ER through the interaction of inositol triphosphate (IP_3) with its receptor (IP_3R)[29]. Upon activation, NFAT migrates from the cytoplasm to the nucleus and directly binds to promoter regions on the JCPyV genome to initiate transcription[28]. Inhibition of calcineurin utilizing the chemical inhibitor Cyclosporine a (CsA), results in a significant reduction in JCPyV infection[28]. Manley et al. demonstrated the importance of NFAT binding to JCPyV DNA to promote transcription of both the early and late viral genes. While these findings suggest the importance of NFAT regulation in JCPyV infection, the role of the IP_3R signaling cascade in NFAT activation during JCPyV infection remains uncharacterized.

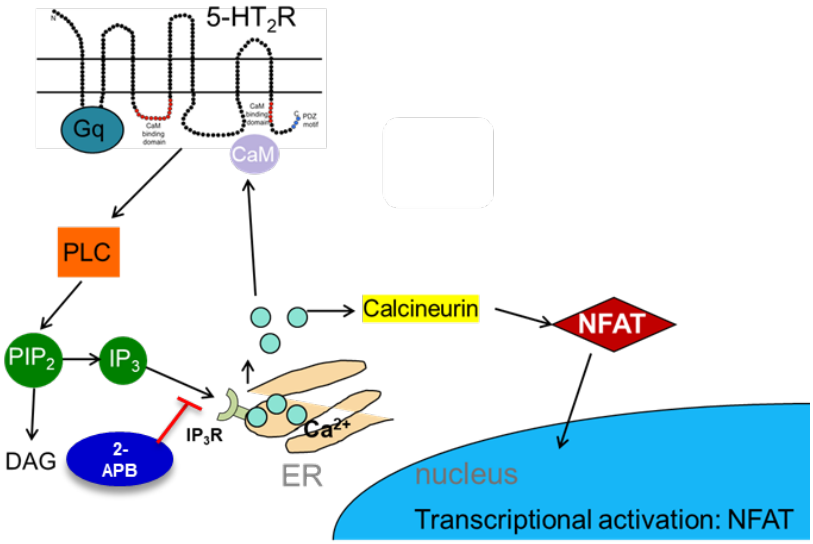

Figure 4. 5-HT_2R-activation of Ca^{2+}/CaM signaling pathway. Activation of 5-HT_2R leads to IP_3 activation of the IP_3R causing a release of Ca^{2+} from the ER, leading to the activation of calmodulin (CaM), which then binds to specific sites on the intracellular loops on the 5-HT_2R, and/or calcineurin, which activates nuclear factor of activated T cells (NFAT), a transcription factor required for JCPyV infection. Inhibition of IP_3R was accomplished utilizing the competitive inhibitor, 2-APB.

IP_3R-mediated calcium signaling

While the role of 5-HT_2Rs in JCPyV entry and infection are not completely understood, it is known that ligand activation of 5-HT_2Rs can activate multiple signaling cascades, which have been observed to regulate the JCPyV lifecycle[20]. The 5-HT_2R recruits calmodulin (CaM), which activates phospholipase C (PLC) and hydrolyses PIP_2 into IP_3 and diacylglycerol (DAG)[29]. Free IP_3 binds to its receptor (IP_3R) which is imbedded within the ER membrane and elicits a flux of calcium ions (Ca^{2+}) into the cytoplasm. Increased cytoplasmic Ca^{2+} then becomes a universal regulator for a multitude of signaling cascades within a cell including activation of calcineurin, a seine/threonine phosphatase that regulate the activation of host transcription factors like NFAT and cellular proliferation (Figure 4)[45]. Additionally, the free Ca^{2+} may bind to CaM and result in binding to intracellular binding domains on the 5-HT_2R, which stabilizes its expression on the exterior of the cell.

Recent studies suggest that viruses have evolved to elicit the release of ER Ca^{2+} stores to drive various stages in their reproductive lifecycles. For example, the human immunodeficiency virus (HIV) is an enveloped, negative-stranded RNA virus that utilizes IP_3R-mediated Ca^{2+} flux to localize Gag, viral structural proteins responsible for virion maturation, to the plasma membrane[30]. At the membrane, Gag mediates viral egress via endocytic sorting complex required for transport (ESCRT)[31]. Meanwhile, Dengue virus (DENV), an enveloped, positive-stranded RNA virus, induces Ca^{2+} flux from the ER to initiate store-operated Ca^{2+} entry (SOCE) to drive viral replication[32]. Furthermore, coxsackievirus B (CVB) is a nonenveloped, positive-sense RNA virus that utilizes IP_3R-mediated Ca^{2+} flux to induce vacuolization of cells, which mediates viral

internalization and trafficking through the cell[33]. While these viruses have different physical structures, genomes, and egress strategies, they are all unified in their dependence on intracellular Ca^{2+} to drive infection. Based on the viral-induced Ca^{2+} flux pathways elicited by a wide-range of viruses and JCPyV activation of potential Ca^{2+}-driven signaling pathways through 5-HT_2Rs[22], MAPK[26], and NFAT[28], it is hypothesized that JCPyV also depends on IP_3R-mediated Ca^{2+} release to drive the infectious viral lifecycle.

Research goals

The goal of this thesis research was to define the role of IP_3R-mediated intracellular Ca^{2+} flux from the ER in regulating JCPyV infection. Studies using an ER-specific Ca^{2+} reporter assay to track Ca^{2+} levels within the ER, suggest that JCPyV infection induces the release of ER Ca^{2+} stores at 2 h post infection. To determine whether Ca^{2+} flux is necessary for JCPyV infection, an IP_3R chemical inhibitor was utilized and resulted in a dose-dependent-decrease in both viral VP1 and T Ag expression. JCPyV-induced Ca^{2+} flux within 0-3 h following viral infection, times that are consistent with viral attachment and entry. To elucidate the step in the virus lifecycle affected by the inhibition of Ca^{2+} flux, JCPyV attachment and internalization were examined. However, data revealed that treatment with the IP_3R inhibitor had no effect on viral attachment or entry when compared to untreated cells. Together, these results suggest that JCPyV activates Ca^{2+} flux upon infection, and Ca^{2+} flux regulates JCPyV infection at a post-entry step in the virus lifecycle.

These data provide researchers with greater insight into the JCPyV infectious lifecycle and helps to increase our general understanding of the viral-host cell interactions

that impact human disease. Additionally, these experiments increase our understanding of the importance of Ca^{2+} signaling in viral infections within the field of virology. It is possible that this information may provide the insights necessary to identify novel targets for antivirals therapies for populations at risk of developing the fatal disease PML.

MATERIALS AND METHODS

Cell culture maintenance

Cell culture experiments were conducted utilizing Lab Gard II laminar flow hoods to maintain a sterile environment. SVG-A (human fetal glial cells transformed with SV40 T antigen) and human embryonic kidney cell lines that stably express 5-HT_{2A}R (HEK293A-5-HT_{2A}R) were generously provided from Dr. Walter Atwood's laboratory (Brown University). Cells were maintained in T75 flasks and were grown in a humidified incubator at 37°C with 5% CO_2. Cell lines were passaged upon visually reaching 90% confluency, as observed using a light microscope. SVG-A cells were cultured in Minimum Essential Medium (MEM) with 10% fetal bovine serum (FBS), 1% penicillin/streptomycin (P/S) (Mediatech, Inc.), and 0.2% plasmocin (Invivogen). HEK293A-5-HT_{2A}R cells were cultured with Dulbecco's Modified Eagle Medium (DMEM) with the same concentrations of FBS, P/S, and plasmocin. For subculturing, cells were detached from flasks with 4 mL of 0.5% trypsin-EDTA (Gibco, Thermo Fischer Scientific) and incubated at 37°C for 5 mins. Following incubation, 9 mL of fresh media was added and transferred to a 15 mL conical tube. The cell suspension was centrifuged at 2,000 rpm for 5 min. Media was aspirated off the pelleted cells, which were then resuspended in 10 mL of fresh complete media and divided into a new flask for continued growth. The new T75 was incubated in a humidified incubator at 37°C and 5% CO_2 until confluency was reached again.

Inhibition of Calcium Flux

2-APB Treatment of SVG-A cells: Wells of a 24-well plate (Grenier Bio-One) were seeded with 2.4e5 cells/well in complete MEM and incubated in a humidified incubator at 37ºC overnight (O/N). Once cells reached ~80% confluency by visual inspection, media was removed, and the 2-APB (Sigma-Aldrich) inhibitor, a competitive inhibitor of the IP_3R, was added in complete MEM with a final volume of 1 mL/well (concentrations specified in Figure Legends). Cells were then incubated at 37ºC for 2 h and then infected (described below).

2-APB Treatment of HEK293A-5-HT2AR cells: Wells of a 24-well plate (Grenier Bio-One) were seeded with 2.4e5 cells/well in complete MEM and incubated in a humidified incubator at 37ºC O/N. Once cells reached ~80% confluency by visual inspection, media was removed, and the 2-APB inhibitor, a competitive inhibitor of the IP_3R, was added in complete MEM with a final volume of 1 mL/well (concentrations specified in Figure Legends).

Xestospongin C treatment of SVG-A cells: Wells of a 24-well plate (Grenier Bio-One) were seeded with 2.4e5 cells/well in complete MEM and incubated in a humidified incubator at 37ºC O/N. Once cells reached ~80% confluency by visual inspection, media was removed, and the Xestospongin C inhibitor, an inhibitor of the IP_3R, was added in complete MEM with a final volume of 1 mL/well (concentrations specified in Figure Legends). Cells were then incubated at 37ºC for 30 min and then infected (described below).

U73122 Treatment of SVG-A cells: Wells of a 24-well plate (Grenier Bio-One) were seeded with 2.4e5 cells/well in complete MEM and incubated in a humidified incubator

at 37°C O/N. Once cells reached ~80% confluency by visual inspection, media was removed, and the inhibitor U73122, which targets PLC, was added in complete MEM with a final volume of 1 mL/well (concentrations specified in Figure Legends). Cells were then incubated at 37°C for 24 h and then infected (described below).

Cellular Proliferation Assay (MTS)

To determine cytotoxic effects of chemical inhibitors, wells in a 96-well plate (Grenier Bio-One) were seeded with 1e4 cells/well in complete MEM and incubated at 37°C O/N. Once cells reached 80% confluency they were treated with the selected chemical, after which fresh media was added to a final volume of 100 µL per well. A volume of 20 µL of the MTS/PMS solution was then added, and cells were incubated at 37°C for 1 h. Post incubation, absorbance was recorded at 490 nm utilizing a BioTek Synergy2 plate reader. The average absorbances were calculated and compared to untreated cells at selected timepoints.

JCPyV infection

Cells that were pretreated with a chemical, control, or transfected with ER-GCaMP had media removed prior to infection. Cells were inoculated with JCPyV in fresh media (multiplicity of infections (MOIs) specified in Figure Legends). Viral infections were conducted in either complete MEM for chemical inhibitors, or phenol red-free complete MEM for ER-GCaMP transfected cells as specified. Cells were incubated with viral inoculums of 200 µL for 24-well plate and 40µL for a 96-well plate for 1 h incubation at 37°C, then cells were fed with 1 mL of complete MEM for a 24-well plate (Grenier Bio-One), or 60 µL for a 96-well plate (Grenier Bio-One). Cells that were being examined for

T Ag expression were incubated for 48 hpi while those being examined for VP1 incubated for 72 hpi.

Fluorescence Focus Assay (FFA)

Following infection, cells were washed with 1 mL of 1XPBS then fixed in ice cold methanol. Fixed cells were then incubated at -20^{o}C for at least 10 mins, washed three times for 10 mins with 1XPBS, and then permeabilized with PBS-0.5% TX100 during a 15-min incubation.

T Ag Staining: Following permeabilization, cells were blocked with 10% goat serum in 1XPBS at RT for 45 min. Cells were then stained for presence of T Ag utilizing the primary PAB692 (1:50) and incubated at 37^{o}C for 1 h (generously provided by the Tevethia lab, Penn State). Cells were washed with 1XPBS Tween (0.01%) three times at RT for 5 min. An anti-mouse Alexa Fluor-594 secondary antibody was used to detect the primary antibody, and cells were incubated at 37^{o}C for 1 h. Finally, cells were washed with 1XPBS three times at RT for 5 min, then stored in 1XPBS Tween (0.01%) at 4^{o}C prior to visualization and quantitation.

VP1 Staining: Following permeabilization, cells were blocked with 10% goat serum at RT for 45 min. Cells were stained with a primary antibody PAB597 (1:10), a hybridoma supernatant, which produces a monoclonal antibody for JCPyV VP1 (provided by Ed Harlow), and incubated at 37^{o}C for 1 h. Cells were washed with 1XPBS three times at RT for 5 min. An anti-mouse Alexa Fluor-488 secondary antibody (1:1000) (Thermo Fisher Scientific) was used to detect the primary antibody and incubated at 37^{o}C for 1 h. Finally, cells were washed with 1XPBS three times at RT for 5 min and then stored in 1XPBS Tween (0.01%) at 4^{o}C prior to visualization and quantitation.

Quantification: Cells were quantified for infectivity via epifluorescence microscopy by counting $VP1^+$ cells in at least 5 visual fields per well in triplicate wells for 3 separate experiments. Expression of VP1 was observed under a 10x objective for a 24-well plate or 20x for a 96-well plate using a Nikon Eclipse Ti epifluorescence microscope. The total number of cells/visual field was quantified by staining cellular DNA with DAPI. DAPI positive cells were quantified using a binary created in the Nikon NIS-Elements Basic Research software (Version 4.5), which controls for equal diameter and circularity of $DAPI^+$ nuclei based upon threshold fluorescence. The percentage of infected cells was calculated by dividing $VP1^+$ cells by the total number of cells, and then normalizing values to the negative control (i.e. DMSO).

Flow cytometry to measure JCPyV attachment

SVG-A cells were cultured to 100% confluency in 6-well plates (Grenier Bio-One) and were treated with a DMSO control or 2-APB (300 μM) in complete MEM at 37°C for 2 h. Cells were then removed from plates by washing with 1XPBS, then incubated with Cellstripper (Corning). SVG-A cells were pelleted at 376 x g at 4°C for 5 min and washed in 1XPBS. Cells were incubated with Alexa-488 fluorescently labeled JCPyV (JCPyV-488) in PBS (100 μL total volume) on ice for 2 h, agitating every 15 min. Following incubation, cells were washed and pelleted by centrifugation before being resuspended in a final volume of 500 μL of 1XPBS. Viral attachment (JCPyV-488) was examined utilizing a BD LSRII (BD Biosciences) with a 488 laser excitation line (Benton, Dickinson, and Company). Data were analyzed based upon 10,000 events using BD FACSDIVA (Benton, Dickinson, and Company) and FlowJo software (Tree Star, Inc.).

Trypan blue quenching assay

SVG-A cells were plated to 100% confluency in 6-well plates (Grenier Bio-One) and pretreated with complete MEM containing either DMSO control or 2-APB (300 μM) at 37°C for 2 h. Cells were then harvested by washing cells with 1XPBS, then incubated with Cellstripper (Corning) at 37°C for 5 min. Cells were centrifuged at 375 x g at 4°C for 5 min. The pellet was washed with 1XPBS, cells were pelleted again, and finally resuspended in phenol-free complete MEM and chilled at 4°C for 30 min. Cells were pelleted and resuspended with JCPyV-488 and incubated at 4°C for 1.5 h with agitation every 15 min. Post incubation, cells were resuspended with cold phenol-free complete MEM and were either fixed (attachment) or incubated at 37°C for 90 min (entry). At 0 or 90 min post-incubation, cells were pelleted and resuspended in 4% PFA on ice for 10 min. Cells were then washed and resuspended in 1XPBS or 1XPBS with Trypan blue (0.016%) in a final volume of 500 μL. Addition of Trypan blue to pre-treated JCPyV-488 incubated cells quenches extracellular fluorescence. Therefore, only internalized JCPyV-488 would remain detectable to the flow cytometer. Analysis for viral internalization was completed utilizing a BD LSRII equipped with a 488 laser line. Data were analyzed with BD FACSDIVA (Becton, Dickinson and Company) and FlowJo software (Tree Star, Inc.). Quenched (addition of Trypan blue) and protected samples (without Trypan blue) from DMSO- and 2-APB-treated cells were assessed by flow cytometry to determine viral attachment (incubation at 4°C only) and viral internalization (incubation at 37°C). Percent protected fluorescence of average FITC readings from quenched and protected samples were calculated by normalizing the mean fluorescence to cells alone. Three samples were examined for each condition, with each sample containing 10,000 events.

ER-GCaMP assay

SVG-A cells were plated 5e3 cells/well in a 96-well black chimney, clear bottom plate (Grenier Bio-One) and incubated O/N at 37^{o}C in complete MEM. Cells were then transfected with a plasmid containing the ER-GCaMP (provided by Drs. Tim Ryan and Julie Gosse) with Fugene6 (Promega) at a 0.2µg of DNA to 0.6µL of Fugene6 in a volume of 10 µL/well in phenol-free complete MEM. Cells were incubated at 37^{o}C for 24 h. The transfection treatment was then removed and replaced with complete MEM and incubated at 37^{o}C for 48 h. Cells were then washed with a Tyrode's buffer (pH 7.4) at 37^{o}C for 30 min. Cells treated with ionomycin or Tyrode's buffer immediately before analysis every 45 sec for 1h (excitation 485/20 and emission 528/20) using a BioTek Synergy2 plate reader with Gen5 (version 5.0). Other cells were infected with JCPyV in Tyrode's buffer at a MOI 0.5 FFU/cell and read every min for 3 h (excitation 485/20 and emission 528/20) using a BioTek Synergy2 plate reader with Gen5 (version 5.0). Readings were normalized to non-transfected or uninfected samples.

Statistical Analysis

Significance was determined utilizing the Microsoft Excel student's paired t-test for at least triplicate samples. *P* values of < 0.05 were considered statistically significant.

RESULTS

JCPyV directly induces Ca^{2+} flux from the ER

Viral-host cell interactions that occur during viral attachment can induce Ca^{2+} flux from the ER to drive viral processes such as internalization, trafficking, replication, and egress by activating critical proteins[31]. The role of JCPyV-induced Ca^{2+} flux has remained unclear, yet recent studies have shown that ERK[26] and NFAT[28], which can also be regulated by IP_3R-mediated Ca^{2+} release, are critical modulators of the JCPyV infectious lifecycle. To examine whether Ca^{2+} release occurs during JCPyV infection, an assay was developed to measure ER- specific Ca^{2+} release in SVG-A cells, a glial cell line optimized for studies of JCPyV infection. SVG-A cells were transfected with a plasmid containing the sequence for a molecular reporter of ER-specific Ca^{2+} signaling, ER-GCaMP. The molecule consists of an enhanced green fluorescent protein (GFP) synthetically attached to a CaM and M13 peptide, both of which act as Ca^{2+} binding domains, with an ER localization signal[34]. ER-GCaMP can only be excited and emit a signal when bound to Ca^{2+} ions within the ER. Emission is detected via plate reader and measured as relative

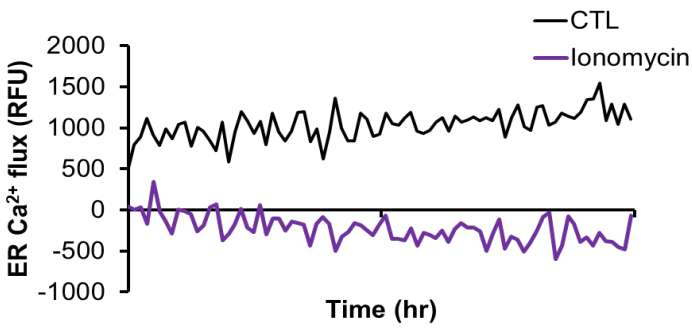

Figure 5. ER-GCaMP is efficient for examining ER Ca^{2+} flux. SVG-A cells were transfected with an ER-GCaMP plasmid and incubated for 48 h. Cells were then treated with ionomycin. At selected time points, cells were analyzed for fluorescence intensity with a BioTek plate reader at 37ºC every 45 sec for 1 h to determine relative fluorescence units (RFUs). Data are representative of three experiments completed with three samples per treatment. ER-GCaMP is efficient for examining ER Ca^{2+} flux.

fluorescence units (RFUs). Therefore, changes in fluorescence measurements represent the relative levels of Ca^{2+} within the ER.

To determine the sensitivity of the assay, transfected cells were examined for RFUs over the course of 1 h after adding ionomycin, a Ca^{2+} ionophore, or a CTL (DMSO) to the cells (Figure 5). Results showed a stable expression of RFUs in the CTL-treated cells for the duration of the experiment while those treated with ionomycin showed a complete abolishment of relative fluorescence units immediately upon addition. These results therefore indicate that this assay is sensitive enough to detect variations in ER Ca^{2+} concentrations. Next, to determine the effect of JCPyV infection on Ca^{2+} flux, cells were mock infected (uninfected) or infected. Fluorescence was recorded for six samples every min for 3 h. Mock-infected cells retained a stable expression of RFUs throughout the duration of the experiment, while the

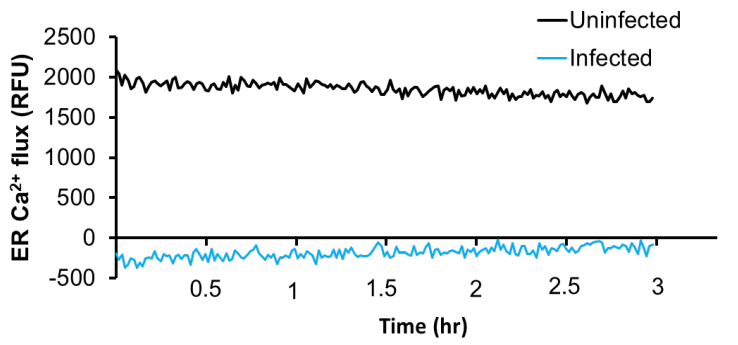

Figure 6. JCPyV induces Ca^{2+} release from ER. SVG-A cells were transfected with an ER-GCaMP plasmid and incubated for 48 h. Cells were then infected with JCPyV (MOI = 0.5 FFU/cell). At selected time points, cells were analyzed for fluorescence intensity with a BioTek plate reader at 37ºC every min for 3 h to determine relative fluorescence units (RFUs). Data are representative of three experiments completed with six samples per treatment. JCPyV infection induces ER Ca^{2+} release.

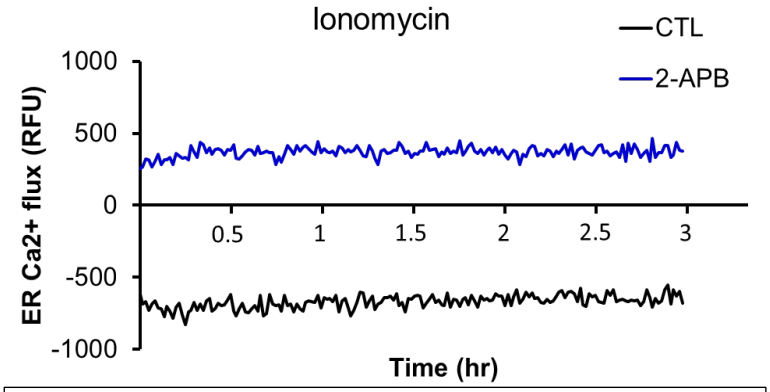

Figure 7. 2-APB is efficient for inhibiting ER Ca^{2+} flux. SVG-A cells were transfected with an ER-GCaMP plasmid and incubated for 48 h. Cells were pretreated for 2-APB or CTL (DSMO) then treated with ionomycin. At selected time points, cells were analyzed for fluorescence intensity with a BioTek plate reader at 37ºC every 45 sec for 1 h to determine relative fluorescence units (RFUs). ER-GCaMP is efficient for examining ER Ca^{2+} flux.

infected cells showed a complete abolishment at the time of infection (Figure 6). These results therefore suggest that JCPyV host-cell interactions are capable of eliciting an ER Ca^{2+} during infection, presumably as early at the viral attachment and entry[5,12,22].

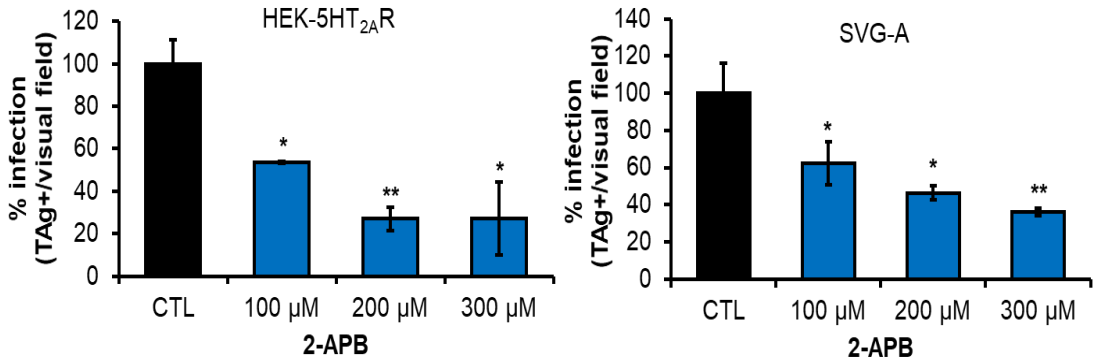

Figure 8. Pretreatment of cells with 2-APB inhibits nuclear expression of TAg. A) HEK-5-HT_{2A}R cells were treated for 1 h or **B)** SVG-A cells were treated for 2 h with either a control (CTL) or 2-APB at 37ºC and then infected with JCPyV at a MOI of 0.1 FFU/cell. Cells were fixed, stained, and quantified for TAg expression by indirect immunofluorescence microscopy. Data represent the average percent infection for 3 visual fields for triplicate samples. Experiment was completed once in triplicate. Error bars represent the SD. *, P<0.03 and **, P<0.005, and ***P<0.005. Treatment with 2-APB reduces JCPyV infection.

IP_3R-mediated Ca^{2+} flux is required for JCPyV infection

While the ER-GCaMP studies revealed that JCPyV infection results in a release of ER Ca^{2+} stores at times consistent with viral attachment and entry, the role of Ca^{2+} flux on the JCPyV infectious cycle was unclear. Upon release from the ER, free Ca^{2+} ions act as ubiquitous secondary regulators for cellular functions[35]. Other viruses including HIV, influenza virus, and Dengue virus have been shown to induce Ca^{2+} flux from the ER to drive various steps in their infectious processes[31,32]. Therefore, to examine the effect of ER Ca^{2+} flux inhibition, cells were pretreated with various chemical inhibitors of the IP_3R-mediated Ca^{2+} release signaling cascade to examine their effect on JCPyV infection. The competitive inhibitor of the IP_3R, 2-APB[36] (Figure 4), was tested for efficacy by determining whether it could inhibit Ca^{2+} flux from the ER utilizing the ER-GCaMP assay. Results showed that cells pretreated with 300 µM of 2-APB compared to CTL-

treated cells retained higher relative fluorescence when treated with ionomycin (Figure 7). These results therefore suggest that 2-APB is efficient at inhibiting Ca^{2+} flux from the ER.

To further characterize whether Ca^{2+} flux is required for JCPyV infection, the kidney cell line HEK293A that stably express 5-$HT_{2A}R$[22] (HEK-5-$HT_{2A}R$) and the glial cell line SVG-A cells were pretreated with 2-APB at indicated concentrations for 2 h, then infected with JCPyV. Infection was quantified using a fluorescence focus assay (FFA) of viral infectivity. Treatment of SVG-A cells with 2-APB lead to a dose-dependent decrease in nuclear expression of both the early gene product T Ag (Figure 8) and late gene product VP1 (Figure 9). Additionally, SVG-A cells were pretreated with Xestospongin C, another competitive inhibitor of the IP_3R, and then examined by FFA for VP1 expression (Figure 10). These results indicated a significant decrease of ~20% in viral infection, thereby corroborating with the 2-APB results (Figure 10). Given that PLC regulates the production of IP_3 (Figure 4), SVG-A cells were pretreated with a PLC inhibitor (U73122) or DMSO control for 24 h prior to infection. Infectivity was scored using a FFA and cells were examined for VP1 expression. Cells treated with U73122 demonstrated a ~20% decrease in JCPyV infection in comparison to DMSO control-

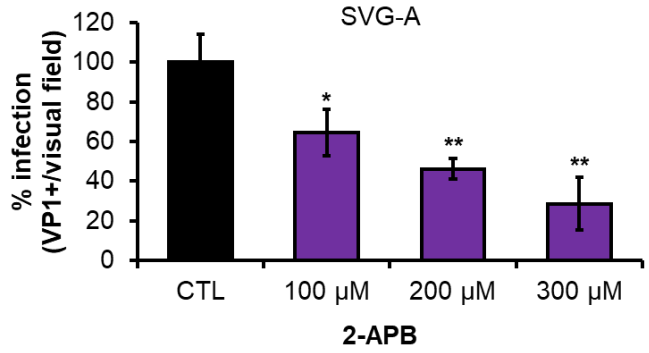

Figure 9. SVG-A cells treated with 2-APB inhibits nuclear expression of VP1. SVG-A cells were treated with either a control (CTL) or 2-APB, an inhibitor of ER Ca^{2+} release, then infected with JCPyV at an MOI of 0.1 FFU/cell at 37°C for 1 h. Cells were fixed, stained, and quantified for VP1 expression by indirect immunofluorescence microscopy. Data represent the average % infection for 3 visual fields for triplicate samples. Data are representative of three experiments completed in triplicate. Error bars represent the SD. *, $P<0.05$ and **, $P<0.005$. Treatment with 2-APB prevented JCPyV infection.

treated cells (Figure 11), suggesting the importance of the IP_3R signaling pathway in JCPyV infection. To ensure chemical treatments were not inducing cellular cytotoxicity, SVG-A cells were subjected to treatments as described in the experimental procedures and a cellular proliferation assay was performed (Figure 12). The concentrations used in these studies did not exhibit cellular toxicity. Together, these data suggest that JCPyV utilizes IP_3R-mediated Ca^{2+} flux from host cell ER stores to drive infection.

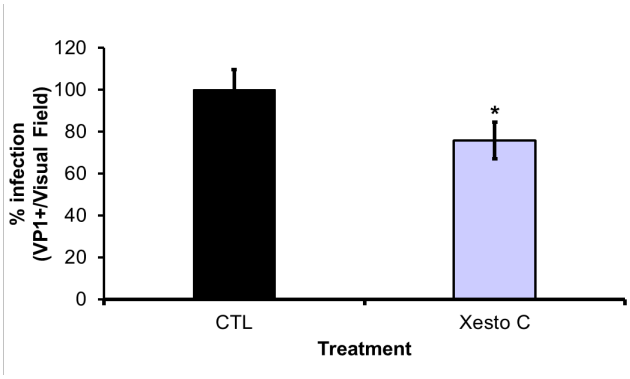

Figure 10. Pretreatment of cells Xestospongin C inhibits nuclear expression of VP1. SVG-A cells were pretreated with either a control (CTL) or Xestospongin C (Xesto C) for 1 h, then infected with JCPyV at an MOI of 0.1 FFU/cell at 37°C for 1 h. Media was added, and cells incubated for 72 h. Post incubation, cells were fixed, stained, and quantified for nuclear VP1 expression indirect immunofluorescence microscopy. The bars represent the average number of infected cells for 3 fields of view for triplicate samples. The error bars represent the SD. Xestospongin C resulted in ~30% decrease in JCPyV infection *, P<0.04

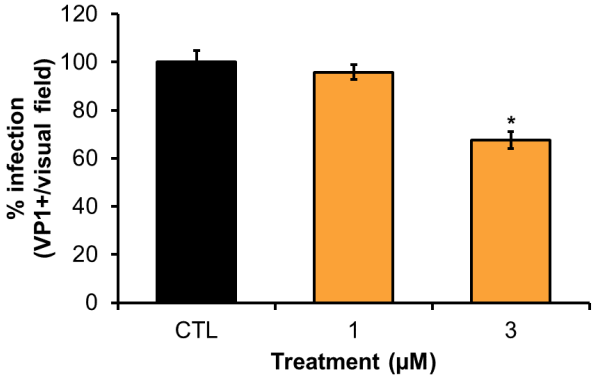

Figure 11. Pretreatment of cells with U73122 inhibits nuclear expression of VP1. SVG-A cells were pretreated with either a control (CTL) or U73122 at 37°C for 24 h, then infected for 1 h. Media was added and cells incubated for 72 h. Post incubation, cells were fixed, stained, and quantified for nuclear VP1 expression indirect immunofluorescence microscopy. The bars represent the average number of infected cells for 3 fields of view for triplicate samples. Experiment was completed three times in triplicate. The error bars represent the SD. U73122 resulted in a dose dependent decrease in JCPyV infection. *, P<0.005.

<u>JCPyV attachment is independent of IP_3R-mediated Ca^{2+} flux</u>

Analysis of Ca^{2+} release from the ER upon JCPyV infection using the ER-GCaMP assay revealed that Ca^{2+} release occurs immediately following infection (0-3 h), and which is a time consistent with viral attachment and entry[5,12,20,22]. To define whether JCPyV depends on IP_3R-mediated Ca^{2+} release from the ER Ca^{2+} flux, viral attachment to cells treated with 2-APB was measured by flow cytometry. SVG-A cells were pretreated with 300

µM of 2-APB, or CTL (DMSO) at 37ºC for 2 h. Cells were detached from plates, suspended, and incubated at 4ºC on ice to induce rigidity in the cell membranes to limit JCPyV internalization. Treated cells were then incubated with an Alexa-488-labeled JCPyV (JCPyV-488) at 4ºC on ice to mediate viral attachment for 90 min[37]. Viral attachment was measured by flow cytometry analysis of the mean fluorescence (JCPyV-488) of 10,000 events per treatment (Figure 13). Results showed no significant change in the mean fluorescence between the 2-APB- or control-treated cells, and that fluorescence is correlated to the presence of JCPyV-488 attachment to SVG-As. These results suggest that inhibition of Ca^{2+} release from the ER with 2-APB treatment does not affect JCPyV binding to host cells. Therefore, it is likely that Ca^{2+} flux regulates a post-attachment step in the JCPyV lifecycle.

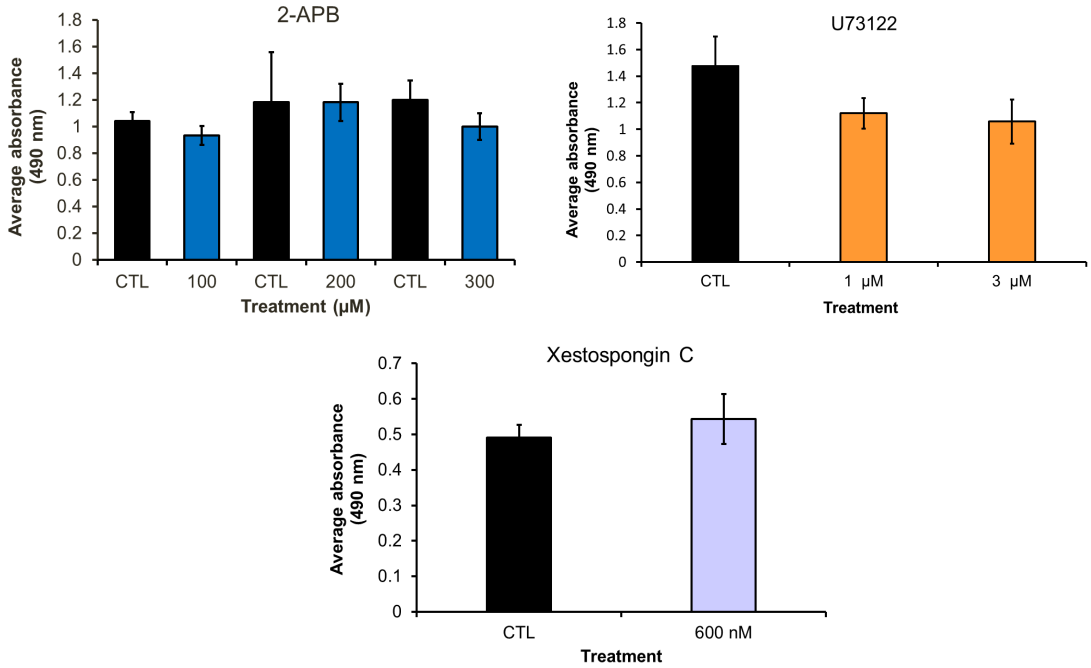

Figure 12. Chemical inhibitors do not affect cellular proliferation. SVGA cells were treated with either a control (CTL) **A)** 2-APB for 2 h, **B)** U73122 for 24 h, or **C)** Xestospongin C for 1h at 37ºC. Post incubation, treatment was removed and replaced with an equivalent volume of media, and cells were incubated at 37ºC for a total of 72 h. MTS was then added to each well and incubated for 1h at 37ºC. Absorbance was measured at 490 nm. Data represent the average absorbance for triplicate samples. Data are representative of three experiments completed in triplicate. Error bars represent SD. Pretreating SVGA cells with 2-APB, U73122, or Xestospongin C does not induce cytotoxicity.

JCPyV internalization is independent of IP_3R-mediated Ca^{2+} flux

Recent data has demonstrated the importance of ER Ca^{2+} signaling in driving viral internalization in the infectious viral lifecycles, including the viral entry step the herpes simplex virus[38]. Further, ER Ca^{2+} flux occurs very early during JCPyV infection (Figure 6), suggesting that Ca^{2+} flux may regulate viral internalization. To determine whether Ca^{2+} flux regulated JCPyV entry, SVG-A cells were pretreated with 300 µM of 2-APB or a CTL (DMSO), and cells were suspended in 1XPBS and incubated at 4°C on ice for 30 mins to induce membrane rigidity. Cells were then incubated with JCPyV-488 in 1XPBS at either at 4°C on ice (attachment) and fixed or shifted to 37°C (entry) for 90 min (Figure 14). Post incubation, cells were washed and treated with or without Trypan blue, which quenches the extracellular Alexa-488 fluorescence while internalized fluorescent molecules are protected from quenching[37]. Triplicate samples were analyzed by flow cytometry (10,000 events for each sample). Data was analyzed to determine the amount of virus that had been internalized (% protected fluorescence), which revealed no change in mean fluorescence between the control- or 2-APB- pretreated SVG-A cells (Figure 14). These results suggest that IP_3R-

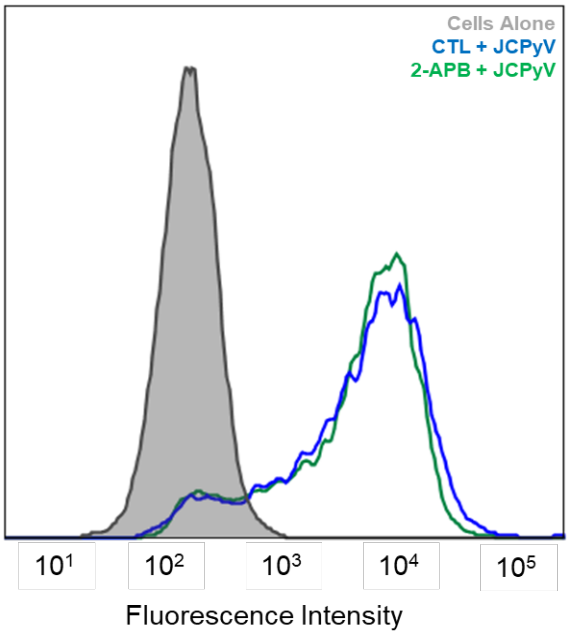

Figure 13. 2-APB does not affect JCPyV attachment to SVG-A cells. To examine viral binding, SVG-A cells were pretreated for 2 h with 2-APB, DMSO (CTL), or PBS (Cells alone) then incubated with fluorescently-labeled JCPyV (JCPyV-488) on ice for 1 h. Cells were analyzed using flow cytometry to detect JCPyV-488. The mean fluorescence intensity was determined for 10,000 events measured. Pretreatment of cells with 2-APB does not impact JCPyV attachment.

mediated Ca^{2+} flux has no effect on JCPyV internalization. Therefore, it is hypothesized that Ca^{2+} flux, which is required for JCPyV infection, affects a post-attachment and post-internalization step in the JCPyV replication cycle.

DISCUSSION

Due the diverse role of Ca^{2+} in cellular signaling, it is defined as a ubiquitous secondary signaling regulator in healthy cells and during times of human disease[35]. Research has shown that specific viral-host cell interactions can elicit Ca^{2+} release from the ER to promote viral infection[27,31,36,38]. Interestingly, Ca^{2+} flux can be initiated upon ligand binding and activation of G-protein coupled receptors (GPCRs), which include the 5-HT_2Rs that are required for JCPyV entry and infection[22,23]. Subsequent signaling cascades are initiated and result in the activation of the IP_3R, a Ca^{2+} ion channel located within the membrane of the ER[39]. This free cytosolic Ca^{2+} is responsible for activating various host transcription factors, proteins involved with endocytosis in addition to dictating cellular proliferation and death, and membrane budding[40].

This research has shown that JCPyV infection results in the release of ER Ca^{2+} at times consistent with viral attachment and entry through a novel application of the ER-GCaMP assay (Figure 6)[20,34]. Additionally, examination of both early and late viral gene products revealed a dose-dependent decrease in viral protein expression in cells pretreated with either an IP_3R or PLC inhibitor. These results suggest that the Ca^{2+} flux regulates a step in the JCPyV infectious cycle prior to transcription (Figure 8-10). However, there was no change in either viral attachment or entry in the presence of the 2-APB inhibitor (Figures 13 and 14), suggesting that Ca^{2+} flux has no effect on JCPyV attachment or entry. Therefore, JCPyV-induced Ca^{2+} flux is hypothesized to regulate a process post viral entry and prior to transcription and has the potential to regulate

multiple steps in the JCPyV infectious cycle, such as trafficking, partial uncoating of the viral capsid, and activation of host transcription factors.

Following internalization, JCPyV is trafficked through the cytoplasm within the endocytic compartment via early endosomes and caveolin-1+ vesicles[25,41]. Early endosome formation and function are closely regulated by Ras-associated binding protein 5 (Rab5)[42]. Rab5 is activated via GTPases that are regulated by GPCRs[43]. Rab5 recruits Rab effector proteins, which are responsible for endosomal fusion and trafficking[42]. As JCPyV has been shown to require a specific family of GPCRs, 5-HT_2Rs, it is possible that their activation not only mediates viral internalization, but also induces ER Ca^{2+} flux to activate Rab5 for early endosomal trafficking. Early endosomal trafficking is a necessary step in the JCPyV lifecycle, which results in delivery of the virus to the ER where the capsid undergoes a partial uncoating[4]. This uncoating process is required for viral deposition into the cytosol and eventual translocation to the nucleus where the viral genome is released for transcription and viral replication[4]. It is therefore possible that modulation of the ER Ca^{2+} release inhibits viral trafficking and therefore reduces viral transcription. This would therefore be consistent

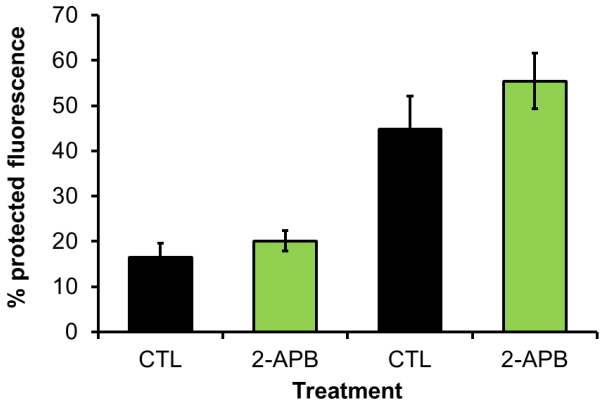

Figure 14. 2-APB does not affect JCPyV entry in SVG-A cells. SVG-A cells were pretreated with 2-APB at 37ºC for 2 h then incubated with fluorescently-labeled JCPyV on ice for 1 h for viral attachment. Cells were treated with or without trypan blue to quench extracellular fluorescence or incubated at 37ºC for 90 min to mediate viral entry and subsequently treated with trypan blue. Internalized virions were protected within the cell and capable of detection using flow cytometry. Pretreatment of cells with 2-APB does not affect JCPyV internalization.

with results showing inhibition of Ca^{2+} flux results in decreased expression of both early and late viral gene products (Figure 8 and 9).

Additionally, it is also possible that IP_3R-mediated ER Ca^{2+} flux, thereby altering the ER's internal environment, is affecting JCPyV capsid uncoating. Research has shown that inhibiting the release of cellular Ca^{2+} stores negatively affects the viral uncoating processes within the ER[37]. Research by Nelson et al. suggests that release of ER Ca^{2+} activates ER-localized enzymes responsible for mediating JCPyV uncoating[37]. Therefore, it is possible that JCPyV induces IP_3R-mediated ER Ca^{2+} to regulate the ERAD pathway and subsequent capsid uncoating within the ER. This Ca^{2+} release would occur early in the JCPyV lifecycle, which is demonstrated through the ER-GCaMP assay examining ER Ca^{2+} in JCPyV infected cells (Figure 6). Failure of JCPyV to partially uncoat in the ER would inhibit the delivery of the viral genome into the nucleus, and therefore inhibit viral transcription. This is also consistent with the reduced expression of both early and late viral gene products when IP_3R-mediated Ca^{2+} release was inhibited with 2-APB (Figure 7).

Furthermore, ER Ca^{2+} flux could affect the activation of the protein kinase C (PKC) signaling pathway, which occurs post-entry and prior to viral transcription in the JCPyV lifecycle[26]. Cytosolic Ca^{2+} is capable of activating PKC, a kinase, which regulates the MAPK signaling pathway[44]. PKC initiates the MAPK cascade by phosphorylating Ras, which leads to the subsequent activation of Raf, MEK, and ERK[44]. Interestingly, the ER-GCaMP results revealed that Ca^{2+} flux occurs immediately upon viral infection. These results interestingly coincide with recent studies showing that the activation of ERK through phosphorylation occurs shortly after JCPyV infection[26]. Interestingly, the

activation of ERK has also been linked to the regulation of NFAT, a molecule known to be a critical regulator in JCPyV transcription and infection[28,45]. Therefore, it is possible that JCPyV induced Ca^{2+} release is promoting viral gene transcription by regulating necessary transcription factors through the activation of PKC.

As Ca^{2+} is defined as a universal secondary regulator, the ion itself would not be a viable target for either JCPyV infection or PML[35]. Inhibition of the ion could result in host cell death and thus lead to serious medical complications. One example is the importance of Ca^{2+} release in neuron activity. In this pathway glutamate activates a GPCR to create IP_3, which then binds to its receptor and induces a Ca^{2+} flux. This calcium flux results in Ca^{2+}-initiated Ca^{2+} release (CICR) and creates action potential within the pacemaker neurons of a human brain[29]. Similarly, Ca^{2+} signaling is also a critical regulator for muscle contraction, including muscles involved in regulating the heart[29]. Thus, it would be better to utilize our understanding of the role Ca^{2+} signaling pathway in regulating JCPyV infection to identify novel targets for JCPyV therapies. As the data has shown that ER Ca^{2+} release fails to inhibit viral attachment or internalization, yet it does have an effect on viral replication, and future research could help identify possible therapeutic targets such as transcription factors (NFAT) or activation of kinases such as ERK that regulate phosphorylation of transcription factors. Currently, there are inhibitors for the phosphatase calcineurin (Cyclosporin A) which regulates NFAT, and U0126 which inhibits ERK activation[26,28]. These could serve as the basis for developing novel therapies.

Additionally, this research has described a new molecular assay sensitive enough to detect changes in Ca^{2+} concentrations within a selected organelle during viral

infection. This assay, along with the Ca^{2+} inhibition assays, has provided deeper insight how viral-host cell interactions regulate JCPyV infection and specifically how IP_3R-mediated Ca^{2+} release regulates viral infection and pathogenesis. These findings can be applied broadly to the field of virology to increase our understanding of viral-induced signaling pathways that drive viral infection, influence viral pathogenesis, and ultimately influence human disease development.

REFERENCES

1. Flint, J., Racaniello, V. R., Rall, G. F. & Anna Marie. *Principles of Virology*. **1,** (ASM Press).

2. Flint, J., Racaniello, V. R., Rall, G. F. & Skalka, A. M. *Principles of Virology*. **II,**

3. Engleberg, N. C., Dirita, V. & Dermody, T. S. *Mechanisms of Microbial Disease*. (Lippincott Williams & Wilkins, 2013).

4. Ferenczy *et al.* Molecular Biology, Epidemiology, and Pathogenesis of Progressive Multifocal Leukoencephalopathy, the JC Virus-Induced Demyelinating Disease of the Human Brain. *Clinical Microbiology Reviews* **25,** 471–506 (2012).

5. Maginnis, M. S., Nelson, C. D. & Atwood, W. J. JC polyomavirus attachment, entry, and trafficking: unlocking the keys to a fatal infection. *J. Neurovirol.* **21,** 601–13 (2015).

6. Assetta, B. & Atwood, W. J. The biology of JC polyomavirus. *Biol. Chem.* **398,** 839–855 (2017).

7. White, M. K. *et al.* Diagnostic assays for polyomavirus JC and progressive multifocal leukoencephalopathy. *Rev. Med. Virol.* **26,** 102–14 (2016).

8. Hirsch, H. H., Kardas, P., Kranz, D. & Leboeuf, C. The human JC polyomavirus (JCPyV): virological background and clinical implications. *APMIS* **121,** 685–727 (2013).

9. Kean, J., Rao, S., Wang, M. & Garcea, R. Seroepidemiology of Human Polyomaviruses. *Plos Pathog* **5,** e1000363 (2009).

10. Borchardt, J. & Berger, J. Re-evaluating the incidence of natalizumab-associated progressive multifocal leukoencephalopathy. *Multiple Scler Relat Disord* **8,** 145–150 (2016).

11. Perkins, M. *et al.* Changes in JC Virus-Specific T Cell Responses during Natalizumab Treatment and in Natalizumab-Associated Progressive Multifocal Leukoencephalopathy. *Plos Pathog* **8,** e1003014 (2012).

12. Neu, U. *et al.* Structure-Function Analysis of the Human JC Polyomavirus Establishes the LSTc Pentasaccharide as a Functional Receptor Motif. *Cell Host Microbe* **8,** 309–319 (2010).

13. Saylor, D. & Venkatesan, A. Progressive Multifocal Leukoencephalopathy in HIV-Uninfected Individuals. *Curr Infect Dis Reports* **18,** 33 (2016).

14. Saribaş, A., Özdemir, A., Lam, C. & Safak, M. JC virus-induced progressive multifocal leukoencephalopathy. *Future Virol* **5,** 313–323 (2010).

15. Berger, J. & Houff, S. Progressive multifocal leukoencephalopathy: lessons from AIDS and natalizumab. *Neurological Research* **28,** 299–305 (2013).

16. Antoniol, C. & Stankoff, B. Immunological Markers for PML Prediction in MS Patients Treated with Natalizumab. *Front Immunol* **5,** 668 (2014).

17. Major, E. O., Amemiya, K., Tornatore, C. S., Houff, S. A. & Berger, J. R. Pathogenesis and Molecular Biology of Progressive Multifocal Leukoencephalopathy, the JC Virus-Induced Demyelinating Disease of the Human Brain. *Clinical Microbiology Reviews* **5,** 49–73 (1992).

18. Safar, A., Rubocki, R. J., Horvath, J. A., Narayan, K. K. & Waldron, R. L. Fatal Immune Restoration Disease in Human Immunodeficiency Virus Type 1-Infected Patients with Progressive Multifocal Leukoencephalopathy: Impact of Antiretroviral Therapy-Associated Immune Reconstitution. *Clinical Infectious Disease* 1250–1257 (2002).

19. French, M. A. *et al.* Immune restoration disease after the treatment of immunodeficient HIV-infected patients with highly active antiretroviral therapy. *HIV Med.* **1,** 107–15 (2000).

20. Mayberry, C., Nelson, C. & Maginnis, M. JC Polyomavirus Attachment and Entry: Potential Sites for PML Therapeutics. *Curr Clin Microbiol Reports* **4,** 132–141 (2017).

21. Gorelik, L. *et al.* Progressive Multifocal Leukoencephalopathy (PML) Development Is Associated With Mutations in JC Virus Capsid Protein VP1 That Change Its Receptor Specificity. *J Infect Dis* **204,** 103–114 (2011).

22. Assetta, B. *et al.* 5-HT2 Receptors Facilitate JC Polyomavirus Entry. *J Virol* **87,** 13490–13498 (2013).

23. Elphick, G. *et al.* The Human Polyomavirus, JCV, Uses Serotonin Receptors to Infect Cells. *Science* **306,** 1380–1383 (2004).

24. Baum, S. *et al.* Early Events in the Life Cycle of JC Virus as Potential Therapeutic Targets for the Treatment of Progressive Multifocal Leukoencephalopathy. *J Neurovirol* **9,** 32–37 (2003).

25. Pho, M. T., Ashok, A. & Atwood, W. J. JC virus enters human glial cells by clathrin-dependent receptor-mediated endocytosis. *J. Virol.* **74,** 2288–92 (2000).

26. DuShane, J., Wilczek, M., Mayberry, C. & Maginnis, M. ERK is a Critical Regulator of JC Polyomavirus Infection. *J Virol* JVI.01529–17 (2018). doi:10.1128/JVI.01529-17

27. Ruiz, M. C., Cohen, J. & Michelangeli, F. Role of Ca2+in the replication and pathogenesis of rotavirus and other viral infections. *Cell Calcium* **28,** 137–149 (2000).

28. Manley, K. *et al.* NFAT4 Is Required for JC Virus Infection of Glial Cells. *Journal of Virology* **80,** 12079–12085 (2006).

29. Berridge, M. Inositol trisphosphate and calcium signalling mechanisms. *Biochimica Et Biophysica Acta Bba - Mol Cell Res* **1793,** 933–940 (2009).

30. Freed, E. O. HIV-1 gag proteins: diverse functions in the virus life cycle. *Virology* **251,** 1–15 (1998).

31. Ehrlich, L., Medina, G. & Carter, C. ESCRT Machinery Potentiates HIV-1 Utilization of the PI(4,5)P2-PLC-IP3R-Ca2+ Signaling Cascade. *J Mol Biol* **413,** 347–358 (2011).

32. Dionicio, C. *et al.* Dengue virus induced changes in Ca2+ homeostasis in human hepatic cells that favor the viral replicative cycle. *Virus Res* **245,** (2018).

33. Bozym, R., Morosky, S., Kim, K., Cherry, S. & Coyne, C. Release of Intracellular Calcium Stores Facilitates Coxsackievirus Entry into Polarized Endothelial Cells. *Plos Pathog* **6,** e1001135 (2010).

34. De Juan-Sanz, J. *et al.* Axonal Endoplasmic Reticulum Ca2+ Content Controls Release Probability in CNS Nerve Terminals. *Neuron* **93,** 867–881.e6 (2017).

35. Nelson, D. L. & Cox, M. M. *Principles of Biochemistry*. (Lehninger, 2013).

36. Bozym, R. *et al.* Calcium signals and calpain-dependent necrosis are essential for release of coxsackievirus B from polarized intestinal epithelial cells. *Mol Biol Cell* **22,** 3010–3021 (2011).

37. Nelson, C., Derdowski, A., Maginnis, M., O'Hara, B. & Atwood, W. The VP1 subunit of JC polyomavirus recapitulates early events in viral trafficking and is a novel tool to study polyomavirus entry. *Virology* **428,** 30–40 (2012).

38. Cheshenko, N. *et al.* Herpes simplex virus triggers activation of calcium-signaling pathways. *J Cell Biology* **163,** 283–293 (2003).

39. Baker, M., Fan, G. & Serysheva, I. Structure of IP3R channel: high-resolution insights from cryo-EM. *Curr Opin Struc Biol* **46,** 38–47 (2017).

40. Chami, M., Oulès, B. & Paterlini-Bréchot, P. Cytobiological consequences of calcium-signaling alterations induced by human viral proteins. *Biochim. Biophys. Acta* **1763,** 1344–62 (2006).

41. Querbes, W., O'Hara, B. A., Williams, G. & Atwood, W. J. Invasion of host cells by JC virus identifies a novel role for caveolae in endosomal sorting of noncaveolar ligands. *J. Virol.* **80,** 9402–13 (2006).

42. Jovic, M., Sharma, M., Rahajeng, J. & Caplan, S. The early endosome: a busy sorting station for proteins at the crossroads. *Histol. Histopathol.* **25,** 99–112 (2010).

43. Murph, M., Scaccia, L., Volpicelli, L. & Radhakrishna, H. Agonist-induced endocytosis of lysophosphatidic acid-coupled LPA1/EDG-2 receptors via a dynamin2- and Rab5-dependent pathway. *J Cell Sci* **116,** 1969–1980 (2003).

44. Webb, B. L., Hirst, S. J. & Giembycz, M. A. Protein kinase C isoenzymes: a review of their structure, regulation and role in regulating airways smooth muscle tone and mitogenesis. *Br. J. Pharmacol.* **130,** 1433–52 (2000).

45. Crabtree, G. R. & Olson, E. N. NFAT signaling: choreographing the social lives of cells. *Cell* **109 Suppl,** S67–79 (2002).

AUTHOR'S BIOGRAPHY

Ashley N. Soucy is from Dunbarton, New Hampshire. Upon graduating from Goffstown High School in 2014, Ashley began pursuing her Bachelor of Science in Biochemistry at The University of Maine. During her four years there, Ashley conducted research in Dr. Melissa Maginnis's laboratory. Ashley received several research fellowships, including the INBRE Functional Genomics Junior and Thesis Fellowships, and was honored to receive the Susan Elliot Judd Roxby Memorial Scholarship. As an undergraduate, Ashley presented her work on the role of Ca^{2+} signaling in JC Polyomavirus infection at thirteen local, regional, and national conferences.

After graduating in 2018, Ashley plans to work as a research assistant before applying for a Ph.D. program in biomedical science. When not in the lab, Ashley enjoys spending time in the outdoors, playing with her dog, and watching Disney movies.